



# Periodontal Regeneration Using Strontium-Loaded Mesoporous Bioactive Glass Scaffolds in Osteoporotic Rats

Yufeng Zhang<sup>1</sup>, Lingfei Wei<sup>1</sup>, Chengtie Wu<sup>2\*</sup>, Richard J. Miron<sup>1,3\*</sup>

**1** The State Key Laboratory Breeding Base of Basic Science of Stomatology (Hubei-MOST) & Key Laboratory of Oral Biomedicine Ministry of Education, Wuhan University, Wuhan, People's Republic of China, **2** State Key Laboratory of High Performance Ceramics and Superfine Microstructure, Shanghai Institute of Ceramics, Shanghai, People's Republic of China, **3** Faculté de médecine dentaire, Université Laval, Québec, Canada

## Abstract

Recent studies demonstrate that the rate of periodontal breakdown significantly increased in patients compromised from both periodontal disease and osteoporosis. One pharmacological agent used for their treatment is strontium ranelate due to its simultaneous ability to increase bone formation and halt bone resorption. The aim of the present study was to achieve periodontal regeneration of strontium-incorporated mesoporous bioactive glass (Sr-MBG) scaffolds in an osteoporotic animal model carried out by bilateral ovariectomy (OVX). 15 female Wistar rats were randomly assigned to three groups: control unfilled periodontal defects, 2) MBG alone and 3) Sr-MBG scaffolds. 10 weeks after OVX, bilateral fenestration defects were created at the buccal aspect of the first mandibular molar and assessed by micro-CT and histomorphometric analysis after 28 days. Periodontal fenestration defects treated with Sr-MBG scaffolds showed greater new bone formation (46.67%) when compared to MBG scaffolds (39.33%) and control unfilled samples (17.50%). The number of TRAP-positive osteoclasts was also significantly reduced in defects receiving Sr-MBG scaffolds. The results from the present study suggest that Sr-MBG scaffolds may provide greater periodontal regeneration. Clinical studies are required to fully characterize the possible beneficial effect of Sr-releasing scaffolds for patients suffering from a combination of both periodontal disease and osteoporosis.

**Citation:** Zhang Y, Wei L, Wu C, Miron RJ (2014) Periodontal Regeneration Using Strontium-Loaded Mesoporous Bioactive Glass Scaffolds in Osteoporotic Rats. PLoS ONE 9(8): e104527. doi:10.1371/journal.pone.0104527

**Editor:** Michael Glogauer, University of Toronto, Canada

**Received:** April 4, 2014; **Accepted:** July 14, 2014; **Published:** August 12, 2014

**Copyright:** © 2014 Zhang et al. This is an open-access article distributed under the terms of the Creative Commons Attribution License, which permits unrestricted use, distribution, and reproduction in any medium, provided the original author and source are credited.

**Funding:** This project was supported by Program for New Century Excellent Talents in University (NCET-11-0414), Excellent Youth Foundation of Hubei and the funds of the National Natural Science Foundation of China (81271108), Shanghai Pujiang Talent Program (12PJ1409500) and Natural Science Foundation of China (Grant 31370963). The funders had no role in study design, data collection and analysis, decision to publish, or preparation of the manuscript.

**Competing Interests:** The authors have declared that no competing interests exist.

\* Email: richard.miron@zmk.unibe.ch (RM); chengtiewu@mail.sic.ac.cn (CW)

## Introduction

Osteoporosis is a worldwide chronic disease which now affects over 200 million people worldwide characterized by low bone mass, poor bone strength and microarchitectural deterioration of bone [1]. The primary cause is governed by the imbalance between bone forming osteoblasts and bone resorbing osteoclasts commonly resulting from postmenopausal oestrogen deficiency [2,3]. At present, the two major therapies include the use of anabolic agents such as parathyroid hormone that stimulate bone formation, and anti-resorptive agents including bisphosphonates, calcitonin, raloxifene, RANKL inhibitors and estrogen which act by inhibiting osteoclast differentiation and activity [4,5]. In relation to periodontal tissues, osteoporosis is believed to contribute to periodontal breakdown given that it may increase bone resorption and prevent proper healing ultimately increasing the severity of the pre-existing periodontal disease [6–8]. Diminished bone density as seen in osteoporotic bone leads to an increase in susceptibility towards alveolar bone loss and further complicates regenerative periodontal procedures.

One agent that is clinically used to prevent bone loss in osteoporotic patients is strontium ranelate [9–14]. Studies have demonstrated that it simultaneously acts by both increasing bone formation and decreasing bone resorption [15–20] thus demonstrating increases in bone mineral density in the lumbar spine, the femoral neck and in total hip reconstruction following its use in clinical trials [21–25]. Its dual mechanism of action makes it advantageous over other leading therapies. While the great majority of research in the field of osteoporosis is currently focused on the preventative measures of disease progression, less study on the therapeutic effect of local transplantation of bioactive scaffolds has been investigated following osteoporotic-related fractures. The advancements in tissue engineering over the last several decades warrant the discovery and application of new therapeutic options carrying bioactive and pharmacological agents within scaffolds capable of guiding cell tissue response upon implantation.

One bone grafting material that has gained awareness in recent years is mesoporous bioactive glass (MBG); a synthetic bone graft capable of bone regeneration [26,27]. Recently it has been

demonstrated that the chemical composition in MBG (CaO-P2O5-SiO2) improves the *in vitro* cell activity of cells seeded on MBG scaffolds and improves bone osseointegration *in vivo* [28,29]. Furthermore, MBG scaffolds have optimal degradation properties making them slowly resorbed over time and replaced by native bone and provide the additional benefit of easily carrying pharmacological agents capable of being released over time to the surrounding tissues [28–31]. Recently we have demonstrated that the advantages of MBG scaffolds incorporated with trace element Strontium (Sr-MBG) were a suitable scaffold for the delivery of strontium to bone defects in a rat osteoporosis model [30,31]. The aim of the present study was to determine if the advantages of Sr-containing mesoporous bioactive glass scaffolds could also be advantageous for the repair of alveolar bone defects created in periodontal tissues. Acute type fenestration defects were created on the buccal aspect of first mandibular molars in 15 ovariectomized rats to generate an osteoporotic phenotype. Healing was assessed 4 weeks post implantation by micro-CT, hematoxylin and eosin staining, and Mason staining.

## Materials and Methods

### Animals and surgical procedures

15 mature female Wistar rats (10 weeks old, mean body weight 230 g) were purchased and used for this study with all handling and surgical procedure approved by the Ethics Committee for Animal Research, Wuhan University, China. Animals had food and water *ad libitum* with constant temperature at 22 degrees Celsius.

After one week for acclimatizing to the new laboratory surroundings, an osteoporosis animal model was carried out by bilateral ovariectomy (OVX) under sterile conditions with a minimally invasive surgical technique as previously described [32,33]. Briefly, when general anesthesia by intraperitoneal injection of chloral hydrate (10%, 4 ml/kg body weight) was achieved, rats were operated with 10 mm linear bilateral lumbar lateral skin incisions. Then the enterocoelia was exposed by blunt dissection of muscle and peritoneum. The bilateral ovaries were removed gently following ligation of the ovarian artery and vein. Then the overlying muscles and epithelial tissues were sutured in multi-layers. Postoperatively, penicillin (40,000 IU/ml, 1 ml/kg) was injected for 3 days and there was no sign of inflammation or other notable anomaly.

Periodontal fenestration defects (standardized with 2.8 mm in length, 1.4 mm in height and  $\approx$ 0.5 mm in deep) were created 2 months later when an osteoporosis model was established as previously described [34]. Briefly, under general anesthesia, rats were subjected to bilateral extra-oral incision at the base of the mandible. The buccal mandibular bone overlying the first molar roots was removed to create a defect (2.8 mm in length, 1.4 mm in height and  $\approx$ 0.5 mm in depth) using a size-4 round bur. The procedure was performed under an operating microscope to avoid perforation of intraoral mucosa. The roots of the first molar were carefully denuded of their periodontal ligament, overlying cementum, and superficial dentin. The height was standardized to the width of the round bur (diameter 1.4 mm) and extended longitudinally to either side. Then, bilateral defects were created in 15 animals for a total of 30 defects and divided into three groups of 10 defects as follows: 1) non-treated control, 2) MBG alone and 3) Sr-MBG group. Porous strontium-incorporated mesopore-bioglass (Sr-MBG) scaffolds were prepared according to the method as previously described [35]. Following implantation of scaffolds, the

muscle and the skin were repositioned and sutured separately. Postoperatively, penicillin (40,000 IU/ml, 1 ml/kg) was injected intramuscularly for 3 days. Four weeks after surgery, the animals were sacrificed by an overdose of chloral hydrate and samples were removed and prepared for analysis.

### $\mu$ CT analysis

The samples were fixed in 4% formaldehyde for 12 h at 4°C. A  $\mu$ CT imaging system ( $\mu$ CT50, Scanco Medical, Bassersdorf, Switzerland) was used to reveal new bone formation within the defect region. Scanning parameters was performed at 70 kV and 114  $\mu$ A with a thickness of 0.048 mm per slice in medium-resolution mode. For 3D reconstruction, the mineralized bone tissue was differentially segmented with a fixed low threshold (value = 212). Representative sections were cut out from buccal and mesial-distal view. After 3D reconstruction, the bone volume fraction (BV/TV) was determined in defect regions to evaluate new bone formation, using a protocol provided by the manufacturer.

### Histological analysis

The mandibles were decalcified in 10% EDTA for 4 weeks. Gradient dehydration was performed for embedding in paraffin followed by perpendicular sectioning to the long axis of the molar roots as previously described [36]. Serial sections of 5  $\mu$ m were cut and mounted on polylysine-coated slides and then performed for H&E staining, Masson trichrome staining (Sigma #HT15; Sigma-Aldrich, St. Louis, USA.) and tartrate-resistant acid phosphatase (TRAP) staining (Sigma #387A; Sigma-Aldrich, St. Louis, USA.) in accordance with the manufacturer's protocol. For histomorphometry, six individual sections were selected from three different locations, which were situated in the middle, coronal and apical levels of the defect (with 400  $\mu$ m apart from the central). The histometric measurements were determined by processing the images, which were captured with an Olympus DP72 microscope, in Adobe Photoshop CS5 (Adobe Systems, Inc.). New mineralized tissue was identified by Masson trichrome staining and the defect fill was defined as the ratio of area of new mineralized tissue within bony envelope and the total defect area. The number of TRAP-positive cells was performed in a 500  $\mu$ m square of the defect area.

### Statistical analysis

All data analysis was performed using SPSS software and statistically significant values were adopted as  $p < 0.05$ . Based on the sample size, a Kolmogorov-Smirnov Test was used to confirm the asymptotic normality of our data. For the bone density, bone thickness and percentage of angiogenesis, mean and standard deviation (SD) were calculated and statistical inference was made by one-way ANOVA and Student t-test (Newman Keuls Test).

## Results

### Establishment of rat osteoporotic model

Both 2D representation and 3D  $\mu$ -CT images of the ovariectomized rat animal model was confirmed by demonstrating a decrease in trabecular bone volume, thickness and density (Fig. 1). Furthermore, OVX animals also demonstrated a significant increase in trabecular separation, a reduced thickness of cortical bone and enlarged marrow cavities when compared to control animals (Fig. 1). After analysis of 3D reconstruction, BV/TV in the distal femur region was significantly decreased in OVX rats confirming the established osteoporotic model (data not shown).

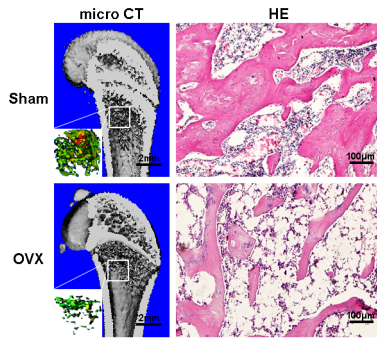


**Figure 1. Establishment of rat osteoporotic model created by OVX.** 3D  $\mu$ -CT images of normal bone and osteoporotic bone as well as their representative H&E staining.  
doi:10.1371/journal.pone.0104527.g001

H&E staining also supported the establishment of an osteoporotic model by demonstrating evident deterioration of trabecular patterns with fat-rich bone marrow-like tissue in ovariectomized rats (Fig. 1).

### 3D reconstruction observations and analysis

Following establishment of an osteoporotic model, representative images of osteogenesis in the periodontal fenestration defect performed by 3D reconstruction for each group were shown in ways of buccal holistic view (Fig. 2 A, D and G) and cutaway view from both horizontal (Fig. 2 B, E and H) and vertical (Fig. 2 C, F and I) directions. Only minimal regenerated bone was visible in the control group, where both defects treated with scaffolds demonstrated newly formed bone following implantation with either MBG or Sr-MBG. The groups receiving Sr-MBG scaffolds exhibited statistically higher newly mineralized tissue when compared to the other modalities (Fig. 3A;  $17.50 \pm 3.94\%$ ,  $39.33 \pm 4.13\%$  and  $46.67 \pm 3.67\%$ ,  $P < 0.01$ , for control, MBG and Sr-MBG, respectively).

### Histological observation and analysis

The histological observation demonstrated that little bone was observed in control defects (Fig. 4A). Within the defects receiving MBG or Sr-MBG scaffolds, a fibrous tissue of woven bone occurred around at the edges as well as around the scaffolds themselves (Fig. 4C and E). Consistently, no new cementum was observed on the root surface among all three groups at a time point of 28 days. It was noted that osteoblasts clustered on the surface of MBG and Sr-MBG and participated aided in the osteogenesis and mineralization (Fig. 4D and F). Noteworthy, more mature alveolar bone was generated around the Sr-MBG when compared to MBG scaffolds. Histomorphometric analysis additionally revealed that the area of new bone was statistically higher in Sr-MBG group ( $0.52 \pm 0.08 \text{ mm}^2$ ) when compared to other modalities (Fig. 3B). Interestingly, little difference was observed between MBG and Sr-MBG for defect fill indicating that the speed of new bone formation was slightly faster in the defects receiving Sr-MBG scaffolds (Fig. 3C).

TRAP-staining was used to determine the number of multi-nucleated cells laying at the edges of the alveolar bone defect in all three groups (Fig. 5). Large multi-nucleated cells stained for TRAP were observed around both MBG and Sr-MBG scaffolds. The

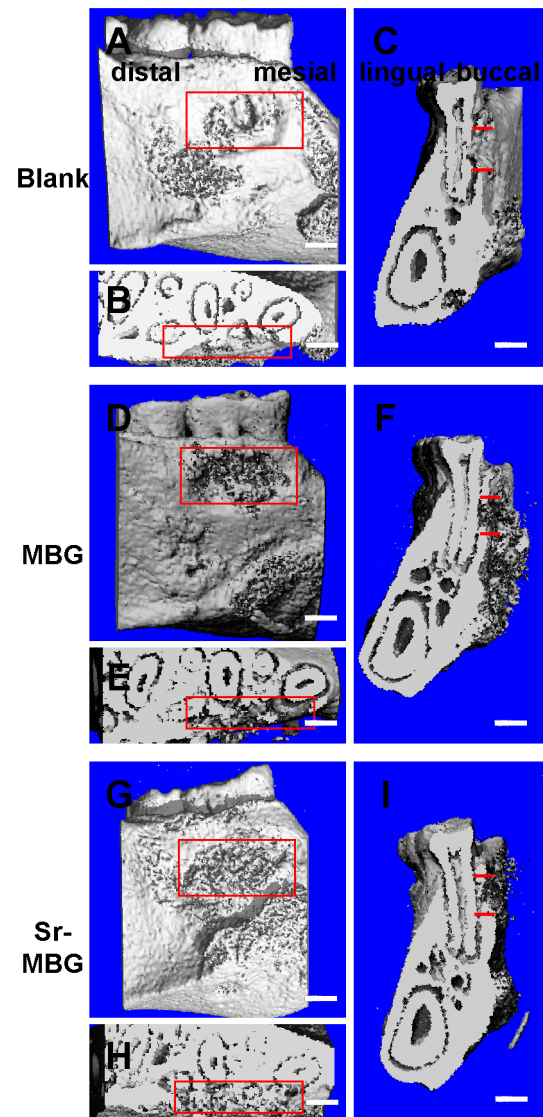


**Figure 2. The overall state of bone regeneration was exhibited by 3D reconstruction.** The red box represented the original extent of surgical defect in general. A, D and G: buccal view; B, E and H: screenshot in horizontal; C, F and I: screenshot in vertical. Bar: 1 mm.  
doi:10.1371/journal.pone.0104527.g002

addition of Sr to MBG significantly decreased the number of TRAP-positive stained cells when compared to MBG scaffolds alone. Both scaffold groups showed higher values when compared to control unfilled defects (Fig. 3D,  $P < 0.01$ ).

### Discussion

The aim of the present study was to investigate the effect of Sr-containing scaffolds on the biological response of periodontal defects created in OVX rats. As the prevalence of osteoporosis continues to rise along with a high number of patients with periodontal disease in the elderly population, the need for treatment modalities directed at patients suffering from precise

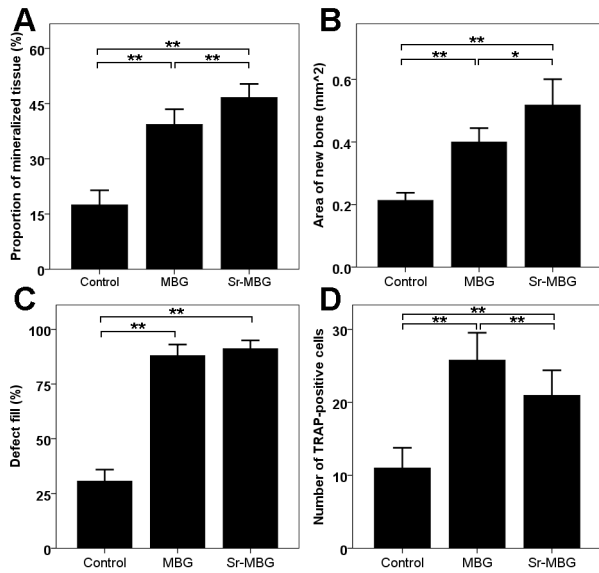


**Figure 3. Statistical analysis of periodontal regeneration: A) proportion of mineralized tissue from horizontal cutaway view of 3D construction, B) area of new bone from H&E stain, C) defect fill from Masson trichrome stain and D) the number of TRAP-positive cells from TRAP stain.** Results were given by mean  $\pm$ SD. \*:  $p < 0.05$ , \*\*:  $p < 0.01$ . doi:10.1371/journal.pone.0104527.g003

combination of diseases remains prominent. The ability to direct therapy to meet the patient’s individual needs remains the clinician’s optimal and desired outcome. For these reasons, the goal of the present study was to utilize the therapeutic benefits from the active pharmacological agent in strontium renalate, and fabricate a scaffold containing Sr to assist in the regeneration of periodontal defects in osteoporotic rats. Recently we have demonstrated that the release kinetics and in vitro behavior of these scaffolds demonstrates ideal release of Sr ions over time and supports osteoblast proliferation and differentiation as well as bone regeneration in a rat femur defect model [31]. The goal therefore of the present study was to further investigate the ability for these scaffolds to fully regenerate the more complicated periodontal defect in OVX animals.

The benefit and future incorporation of Sr into pharmacological agents and biomaterials stems from previous studies indicating that Sr ions is a safe and effective way to stimulate proliferation and differentiation of bone mesenchymal stem cells, osteoblasts and periodontal ligament cells harvested [19,37]. It has previously been demonstrated that Sr significantly influences osteoblastic differentiation by increasing alkaline phosphatase activity, real-time PCR for ALP and osteocalcin mRNA expression, and alizarin red staining for mineralization. Furthermore, recent investigations have also demonstrated a positive correlation of Sr incorporation into biomaterials [38,39].

In order to verify our hypothesis that Sr would be advantage in combination with a carrier scaffold, we created Sr-MBG scaffolds

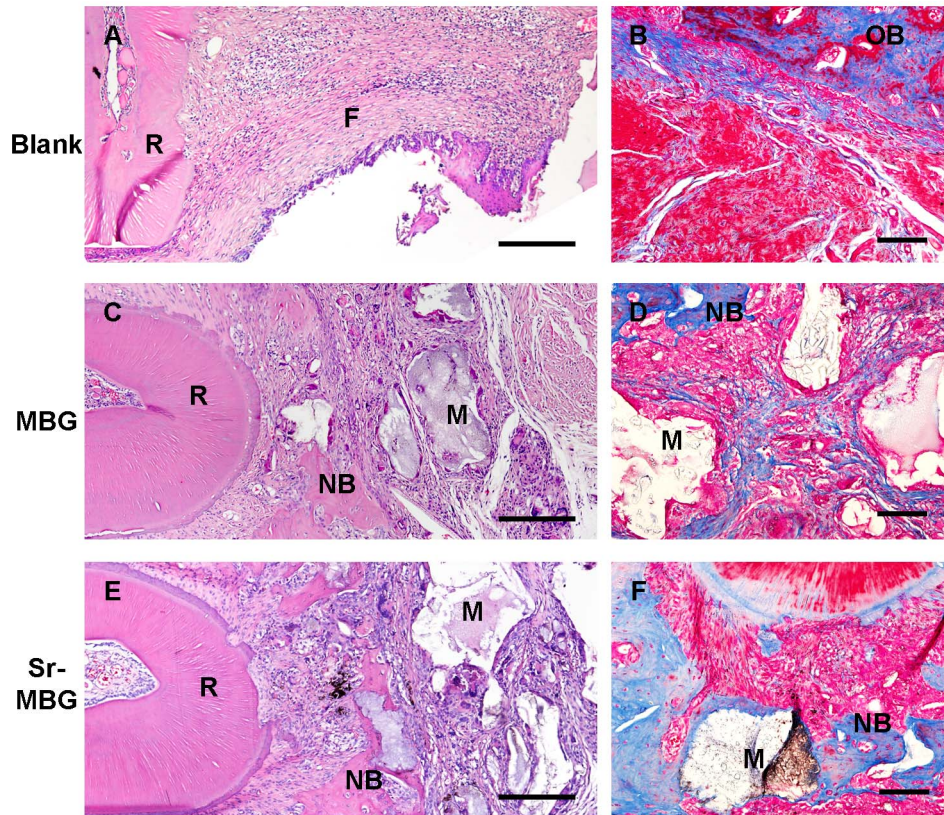


**Figure 4. Representative sections of H&E stain (A, C and E) revealed the osteogenesis among the defects.** New bone was visible in the area adjacent to the old bone and implanted scaffolds. Representative sections of Masson trichrome stain (B, D and F) revealed the compound of collagen in the osteogenic active zone. Bar: 200  $\mu$ m. R: Root, F = Fibroblasts, NB = New bone, OB = Old bone, M = Material. doi:10.1371/journal.pone.0104527.g004

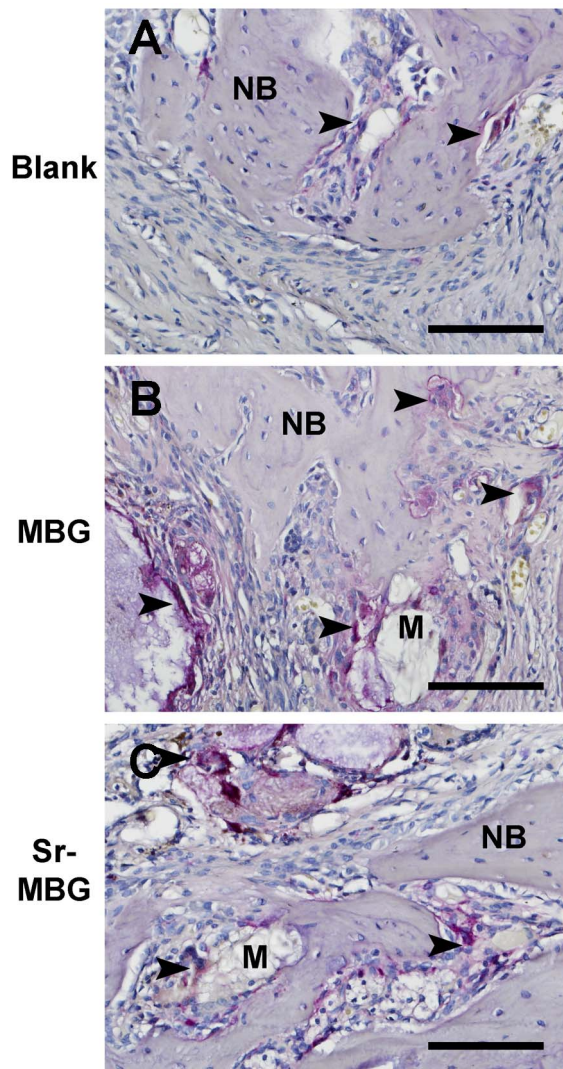


**Figure 5. TRAP-staining for A) control, B) MBG alone and C) Sr-MBG scaffolds.** Positive cells were visible in the surface of bone (control, MBG and Sr-MBG) and scaffolds (MBG and Sr-MBG). Bar: 100  $\mu$ m. Arrows depict areas of TRAP-staining, NB = New bone, M = Material.

doi:10.1371/journal.pone.0104527.g005

and implanted them in acute type periodontal defects in ovariectomised rats to mimic the osteoporotic phenotype. The micro-CT analysis demonstrated that Sr-MBG scaffolds induced more mineralization than MBG scaffolds alone or control samples.

**References**

- Genant HK, Cooper C, Poor G, Reid I, Ehrlich G, et al. (1999) Interim report and recommendations of the World Health Organization Task-Force for Osteoporosis. *Osteoporos Int* 10: 259–264.
- Tontonoz P, Pei LM (2004) Fat’s loss is bone’s gain. *Journal of Clinical Investigation* 113: 805–806.
- Rodan GA, Martin TJ (2000) Therapeutic approaches to bone diseases. *Science* 289: 1508–1514.
- Silva BC, Bilezikian JP (2011) New approaches to the treatment of osteoporosis. *Annu Rev Med* 62: 307–322.
- Boonen S, Ferrari S, Miller PD, Eriksen EF, Sambrook PN, et al. (2012) Postmenopausal osteoporosis treatment with antiresorptives: effects of discontinuation or long-term continuation on bone turnover and fracture risk—a perspective. *J Bone Miner Res* 27: 963–974.

The morphological and histomorphometry analysis based on the HE and Mason staining suggested that the Sr-MBG stimulated a more effectively osteoconductive and anti-osteoporotic phenotype which increased the speed and quality of bone regeneration. Furthermore it was shown from TRAP staining that the number of multi-nucleated giant cells was significantly reduced when Sr was administered in MBG scaffolds (Fig. 4). This finding is in accordance with studies from the literature that demonstrate that Sr is able to suppress osteoclastogenesis [40–44]. It has been shown that Sr is able to reduce osteoclast resorption in vitro [40] by decreasing receptor activator of nuclear factor-KappaB ligand (RANKL)-induced osteoclast differentiation [41,44].

The incorporation of strontium into biomaterials has become a hot topic in recent years. Investigators have now demonstrated positive results for the incorporation of Sr into calcium phosphate [45,46], osseointegration of titanium implants [47,48], hydroxyapatite implants [49–51] and bioactive glass [52]. These investigations utilize the bone formation capabilities of Sr not only for osteoporotic related defects and patients but also for the general public. Thus, it is plausible that the use of Sr may become mainstream within the next decade for a large variety of dental application. The desirable outcome of simultaneously improving bone formation while decreasing bone resorption by incorporating Sr into biomaterials presents many future options for a large variety of applications.

In conclusion, the results from the present study demonstrates that Sr-releasing MBG scaffolds are capable of significantly increasing alveolar bone regeneration in periodontal tissues in OVX rats 28 days post-surgery when compared to control and MBG groups. To the best of our knowledge, we demonstrate for the first time the ability for Sr-containing scaffolds to support bone formation in periodontal tissues in vivo. The scaffolds utilized in this study demonstrate that the release of Sr<sup>2+</sup> ions is capable of improving osteoblast function by increasing new bone formation. Simultaneously, the release of Sr also significantly decreased the number of multi-nucleated osteoclasts as demonstrated by TRAP staining. Taken together, these results suggest that the use of Sr-containing scaffolds may provide greater defect healing in osteoporotic related periodontal defects. Additional clinical studies are required to fully characterize the possible beneficial effect of Sr-MBG scaffolds for patients suffering from both periodontal disease and osteoporosis.

**Author Contributions**

Conceived and designed the experiments: YZ LW CW RM. Performed the experiments: YZ LW CW RM. Analyzed the data: YZ LW CW RM. Contributed reagents/materials/analysis tools: YZ CW. Wrote the paper: YZ LW CW RM.

- Passos Jde S, Gomes-Filho IS, Vianna MI, da Cruz SS, Barreto ML, et al. (2010) Outcome measurements in studies on the association between osteoporosis and periodontal disease. *J Periodontol* 81: 1773–1780.
- Sultan N, Rao J (2011) Association between periodontal disease and bone mineral density in postmenopausal women: a cross sectional study. *Med Oral Patol Oral Cir Bucal* 16: e440–447.
- von Wöwern N, Klausen B, Kollerup G (1994) Osteoporosis: a risk factor in periodontal disease. *J Periodontol* 65: 1134–1138.
- Chung CJ, Long HY (2011) Systematic strontium substitution in hydroxyapatite coatings on titanium via micro-arc treatment and their osteoblast/osteoclast responses. *Acta Biomater* 7: 4081–4087.
- Hao J, Acharya A, Chen K, Chou J, Kasugai S, et al. (2013) Novel bioresorbable strontium hydroxyapatite membrane for guided bone regeneration. *Clin Oral Implants Res*.

11. Gallacher SJ, Dixon T (2010) Impact of treatments for postmenopausal osteoporosis (bisphosphonates, parathyroid hormone, strontium ranelate, and denosumab) on bone quality: a systematic review. *Calcif Tissue Int* 87: 469–484.
12. Marie PJ (2010) Strontium ranelate in osteoporosis and beyond: identifying molecular targets in bone cell biology. *Mol Interv* 10: 305–312.
13. Mentaverri R, Brazier M, Kamel S, Fardellone P (2012) Potential anti-catabolic and anabolic properties of strontium ranelate. *Curr Mol Pharmacol* 5: 189–194.
14. Rizzoli R, Reginster JY (2011) Adverse drug reactions to osteoporosis treatments. *Expert Rev Clin Pharmacol* 4: 593–604.
15. Marie PJ, Ammann P, Boivin G, Rey C (2001) Mechanisms of action and therapeutic potential of strontium in bone. *Calcif Tissue Int* 69: 121–129.
16. Verberckmoes SC, De Broe ME, D'Haese PC (2003) Dose-dependent effects of strontium on osteoblast function and mineralization. *Kidney Int* 64: 534–543.
17. Qiu K, Zhao XJ, Wan CX, Zhao CS, Chen YW (2006) Effect of strontium ions on the growth of ROS17/2.8 cells on porous calcium polyphosphate scaffolds. *Biomaterials* 27: 1277–1286.
18. Peng S, Liu XS, Zhou G, Li Z, Luk KD, et al. (2011) Osteoprotegerin deficiency attenuates strontium-mediated inhibition of osteoclastogenesis and bone resorption. *J Bone Miner Res* 26: 1272–1282.
19. Choudhary S, Halbout P, Alander C, Raisz L, Pilbeam C (2007) Strontium ranelate promotes osteoblastic differentiation and mineralization of murine bone marrow stromal cells: involvement of prostaglandins. *J Bone Miner Res* 22: 1002–1010.
20. Blake GM, Compston JE, Fogelman I (2009) Could strontium ranelate have a synergistic role in the treatment of osteoporosis? *J Bone Miner Res* 24: 1354–1357.
21. Meunier PJ, Slosman DO, Delmas PD, Sebert JL, Brandi ML, et al. (2002) Strontium ranelate: dose-dependent effects in established postmenopausal vertebral osteoporosis—a 2-year randomized placebo controlled trial. *J Clin Endocrinol Metab* 87: 2060–2066.
22. Meunier PJ, Roux C, Seeman E, Ortolani S, Badurski JE, et al. (2004) The effects of strontium ranelate on the risk of vertebral fracture in women with postmenopausal osteoporosis. *N Engl J Med* 350: 459–468.
23. Reginster JY, Seeman E, De Vernejoul MC, Adams S, Compston J, et al. (2005) Strontium ranelate reduces the risk of nonvertebral fractures in postmenopausal women with osteoporosis: Treatment of Peripheral Osteoporosis (TROPOS) study. *J Clin Endocrinol Metab* 90: 2816–2822.
24. Seeman E, Devogelaer JP, Lorenc R, Spector T, Brixen K, et al. (2008) Strontium ranelate reduces the risk of vertebral fractures in patients with osteopenia. *J Bone Miner Res* 23: 433–438.
25. Ammann P, Badoud I, Barraud S, Dayer R, Rizzoli R (2007) Strontium ranelate treatment improves trabecular and cortical intrinsic bone tissue quality, a determinant of bone strength. *J Bone Miner Res* 22: 1419–1425.
26. Yan X, Huang X, Yu C, Deng H, Wang Y, et al. (2006) The in-vitro bioactivity of mesoporous bioactive glasses. *Biomaterials* 27: 3396–3403.
27. Li X, Shi J, Dong X, Zhang L, Zeng H (2008) A mesoporous bioactive glass/polycaprolactone composite scaffold and its bioactivity behavior. *J Biomed Mater Res A* 84: 84–91.
28. Wu C, Ramaswamy Y, Zhu Y, Zheng R, Appleyard R, et al. (2009) The effect of mesoporous bioactive glass on the physicochemical, biological and drug-release properties of poly(DL-lactide-co-glycolide) films. *Biomaterials* 30: 2199–2208.
29. Wu C, Zhang Y, Zhou Y, Fan W, Xiao Y (2011) A comparative study of mesoporous glass/silk and non-mesoporous glass/silk scaffolds: physicochemistry and in vivo osteogenesis. *Acta Biomater* 7: 2229–2236.
30. Wei L, Ke J, Prasadani I, Miron RJ, Lin S, et al. (2014) A comparative study of Sr-incorporated mesoporous bioactive glass scaffolds for regeneration of osteopenic bone defects. *Osteoporos Int*.
31. Zhang Y, Wei L, Chang J, Miron RJ, Shi B, et al. (2013) Strontium-incorporated mesoporous bioactive glass scaffolds stimulating in vitro proliferation and differentiation of bone marrow stromal cells and in vivo regeneration of osteoporotic bone defects. *Journal of Materials Chemistry B* 1: 5711–5722.
32. Cheng N, Dai J, Cheng X, Li S, Miron RJ, et al. (2013) Porous CaP/silk composite scaffolds to repair femur defects in an osteoporotic model. *J Mater Sci Mater Med* 24: 1963–1975.
33. Zhang Y, Cheng N, Miron R, Shi B, Cheng X (2012) Delivery of PDGF-B and BMP-7 by mesoporous bioglass/silk fibrin scaffolds for the repair of osteoporotic defects. *Biomaterials* 33: 6698–6708.
34. Miron RJ, Wei L, Yang S, Caluseru OM, Sculean A, et al. (2014) Effect of an Enamel Matrix Derivative on Periodontal Wound Healing/Regeneration in an Osteoporotic Model. *J Periodontol*: 1–12.
35. Wu C, Zhou Y, Lin C, Chang J, Xiao Y (2012) Strontium-containing mesoporous bioactive glass scaffolds with improved osteogenic/cementogenic differentiation of periodontal ligament cells for periodontal tissue engineering. *Acta Biomater* 8: 3805–3815.
36. Zhao M, Jin Q, Berry JE, Nociti FH, Jr., Giannobile WV, et al. (2004) Cementoblast delivery for periodontal tissue engineering. *J Periodontol* 75: 154–161.
37. Chattopadhyay N, Quinn SJ, Kifor O, Ye C, Brown EM (2007) The calcium-sensing receptor (CaR) is involved in strontium ranelate-induced osteoblast proliferation. *Biochem Pharmacol* 74: 438–447.
38. Han L, Okiji T (2011) Evaluation of the ions release / incorporation of the prototype S-PRG filler-containing endodontic sealer. *Dent Mater J*.
39. Sakai A, Valanezhad A, Ozaki M, Ishikawa K, Matsuya S (2012) Preparation of Sr-containing carbonate apatite as a bone substitute and its properties. *Dent Mater J* 31: 197–205.
40. Bonnelye E, Chabadel A, Saltel F, Jurdic P (2008) Dual effect of strontium ranelate: stimulation of osteoblast differentiation and inhibition of osteoclast formation and resorption in vitro. *Bone* 42: 129–138.
41. Caudrillier A, Hurtel-Lemaire AS, Wattel A, Cournarie F, Godin C, et al. (2010) Strontium ranelate decreases receptor activator of nuclear factor- $\kappa$ B ligand-induced osteoclastic differentiation in vitro: involvement of the calcium-sensing receptor. *Mol Pharmacol* 78: 569–576.
42. Peng S, Liu XS, Huang S, Li Z, Pan H, et al. (2011) The cross-talk between osteoclasts and osteoblasts in response to strontium treatment: involvement of osteoprotegerin. *Bone* 49: 1290–1298.
43. Roy M, Bose S (2012) Osteoclastogenesis and osteoclastic resorption of tricalcium phosphate: effect of strontium and magnesium doping. *J Biomed Mater Res A* 100: 2450–2461.
44. Yamaguchi M, Weitzmann MN (2012) The intact strontium ranelate complex stimulates osteoblastogenesis and suppresses osteoclastogenesis by antagonizing NF- $\kappa$ B activation. *Mol Cell Biochem* 359: 399–407.
45. Baier M, Staudt P, Klein R, Sommer U, Wenz R, et al. (2013) Strontium enhances osseointegration of calcium phosphate cement: a histomorphometric pilot study in ovariectomized rats. *J Orthop Surg Res* 8: 16.
46. Mohan BG, Shenoy SJ, Babu SS, Varma HK, John A (2013) Strontium calcium phosphate for the repair of leporine (*Oryctolagus cuniculus*) ulna segmental defect. *J Biomed Mater Res A* 101: 261–271.
47. Andersen OZ, Offermanns V, Sillassen M, Almqvist KP, Andersen IH, et al. (2013) Accelerated bone ingrowth by local delivery of strontium from surface functionalized titanium implants. *Biomaterials* 34: 5883–5890.
48. Lopa S, Mercuri D, Colombini A, De Conti G, Segatti F, et al. (2013) Orthopedic bioactive implants: Hydrogel enrichment of macroporous titanium for the delivery of mesenchymal stem cells and strontium. *J Biomed Mater Res A*.
49. Yang GL, Song LN, Jiang QH, Wang XX, Zhao SF, et al. (2012) Effect of strontium-substituted nanohydroxyapatite coating of porous implant surfaces on implant osseointegration in a rabbit model. *Int J Oral Maxillofac Implants* 27: 1332–1339.
50. Berglund IS, Brar HS, Dolgova N, Acharya AP, Keselowsky BG, et al. (2012) Synthesis and characterization of Mg-Ca-Sr alloys for biodegradable orthopedic implant applications. *J Biomed Mater Res B Appl Biomater* 100: 1524–1534.
51. Fu DL, Jiang QH, He FM, Yang GL, Liu L (2012) Fluorescence microscopic analysis of bone osseointegration of strontium-substituted hydroxyapatite implants. *J Zhejiang Univ Sci B* 13: 364–371.
52. Brauer DS, Karpukhina N, Kedia G, Bhat A, Law RV, et al. (2012) Bactericidal strontium-releasing injectable bone cements based on bioactive glasses. *J R Soc Interface*.